DOI: 10.13009/EUCASS2023-760
Aerospace Europe Conference 2023 – 10TH EUCASS – 9TH CEAS

# The nanosatellite-class attitude control facility at ESA-ESTEC

*Andrea Curatolo*†, Dario Modenini*, Giacomo Curzi*, Alessandro Lotti*, Daniele Pecorella*, Eliseo Strollo*, Alfredo Locarini**, Andrew Hyslop***, Davide Oddenino****

** Department of Industrial Engineering Alma Mater Studiorum Università di Bologna*

*Via Fontanelle 40, I-47121 Forlì Italy*

*** NautiluS Navigation in Space Srl*

*Via G. Fanin 48, I-40127 Bologna (BO), Italy*

**** European Space Agency – ESTEC*

*Keplerlaan 1, PO Box 299 NL-2200 AG Noordwijk, The Netherlands*

{andrea.curatolo4, dario.modenini, giacomo.curzi2, alessandro.lotti4, daniele.percorella3, eliseo.strollo2} @unibo.it
alfredo.locarini@spacenautilus.com

{andrew.hyslop, davide.oddenino}@esa.int

† Corresponding Author

## Abstract

A facility for testing nanosatellites attitude determination and control systems is under development by the University of Bologna and NautiluS - Navigation in Space, under ESA coordination and funding. The facility, to be installed in ESTEC, will enable the verification of closed-loop attitude control with physical sensor stimulus and physical effects from the actuators driving the dynamics. By testing nanosatellites in such an environment, it is expected to catch issues not identified due to the compressed verification campaign typical of the New-Space approach. The manuscript reports on the project status, focusing on the driving requirements and design choices adopted.

## 1. Introduction

As the number of nanosatellites in orbit is rapidly growing, there is a strong interest in enhancing the reliability of such miniaturized platforms. The CubeSat standard, in particular, is becoming increasingly popular also at ESA, which currently provides technical and financial support for a wide range of technological and scientific missions. Some of these missions, however, suffer failures and/or need prolonged commissioning campaigns to resolve issues with the attitude determination and control system (ADCS) in orbit. A potential mitigation is to provide a verification and validation facility that can truly support a ‘test-as-you-fly’ philosophy [1]. This work describes the development of one such facility, carried out under ESA contract n. 4000140007/22/NL/MGu, to be installed at the AOCS Verification Laboratory in ESTEC.

The ongoing project relies on the experience gathered through a heritage facility developed in the past five years at the µ3S Laboratory at the University of Bologna. At the core of the heritage facility, which allows for testing ADCS of CubeSats in the range from 1U to 3U, is an articulated stand equipped with a table-top air-bearing platform whose function is to hold the mock-up under test and enable an almost frictionless rotational motion. Other subsystems include a Helmholtz cage for geomagnetic field simulation, a Sun simulator, and an in-house developed vision system for ground-truth attitude measurement [2].

The newly designed facility will improve upon its predecessor from several points of view, among which:

- a wider range of CubeSats is supported for testing, from 1U to 12U, allowing them to be placed on the rotating platform in any orientation and ensuring, at the same time, semi-automatic balancing capability;
- the Sun-lamp beam orientation can be adjusted from the overhead position to the horizontal position for testing orbital configurations with solar beta-angles from 0° to 90°.
- An additional lamp will be used to simulate the effect of Earth Albedo
- a higher accuracy ground-truth system is foreseen, whose output may be used, when testing CubeSats equipped with a star tracker, to create a star tracker template model and replace the actual measurements (as long as no optical stimulus is available for such a sensor in the facility).

DOI: 10.13009/EUCASS2023-760



The project started in January 2023 and is expected to end in December 2023 with the integration and commissioning of the facility at ESTEC premises. An acceptance test campaign will also be performed, to ensure that the system meets its expected performance requirements.
This paper reports on the project's current status and presents the main design choices adopted. The main system requirements are presented and serve as a reference for the design choices. The project development has been divided into two main parts, reflecting the facility subsystems: the Air Bearing Table (ABT) development and the Physical Stimulus (PS) development. The former includes the design of the ABT hardware (HW) and software (SW), whose scope is the minimisation of disturbance torque acting on the device under test (DUT), the supply of power to the DUT, and serves as communication relay to the ground station (GS). The latter includes the design of the PS HW and SW, in particular of the magnetic field simulator, the Sun simulator and the ground-truth system. The ABT development is currently in its Manufacturing, Assembly, Integration, and Test (MAIT), while the PS development is currently in its design phase.

### 1.1. Requirements for the facility

The new facility has to comply with a series of requirements formulated by ESA. The facility requirements are divided into 1) General Functional Requirements, 2) Performance Requirements, 3) Sensor Stimulation Requirements, 4) Ground Support Equipment (GSE) Infrastructure Requirements, 5) Installation & Support Requirements. Table 1 displays a subset of the entire requirements list, including those affecting the physical layout, main features and performance indexes of the facility.

**Table 1: Main facility requirements**

| Requirement ID | Requirement text (extract) |
|---|---|
| **General Functional Requirements** | |
| AOC-TB-01 | The facility shall include a spherical air bearing capable of 3 degree-of-freedom attitude motion. |
| AOB-TB-02 | The facility shall be compatible with operating in an ISO 8 class clean room/tent. |
| AOC-TB-03 | The facility shall allow the satellites specified in AOC-TB-15 to be placed on the air bearing mount platform in any orientation where the cubesat is resting on one of its six sides – with mechanical contact only on the rails. |
| AOC-TB-04 | The facility shall include automated mass balancing, with any sensing and actuation independent of the item under test (cubesat), to minimize the efforts to setup a test. |
| AOC-TB-07 | The platform independent orientation measurements (AOC-TB-22) shall be usable in real-time for driving attitude-dependent stimulus |
| AOC-TB-11 | The facility shall include mechanical Ground Support Equipment to allow lifting of 6U and 12U satellites from a transport/storage container onto the air bearing table and supporting their weight during installation on the table. |
| AOC-TB-13 | The facility shall fit into a 2.7 m x 2.7 m x 1.95 m (height) lab space. |
| AOC-TB-14 | The facility shall be re-locatable via wheels at the base that can also be locked via brakes. |
| **Performance Requirements** | |
| AOC-TB-15 | The facility shall support the following cubesat sizes and masses:<br>• 1U (10 x 10 x 11.35 cm, <2 kg)<br>• 3U (10 x 10 x 34.05 cm, <6 kg)<br>• 6U (20 x 10 x 34.05 cm, <12 kg)<br>• 12U (20 cm x 20 cm x 34.05 cm, <24 kg)<br>[as per CubeSat Design Spec., CP-CDS-R14.1]<br>with additional margins of 2 kg and 15 cm per dimension for table- mounted GSE. |
| AOC-TB-16 | The facility shall support the following c.g. offsets from the geometric cubesat center point:<br>• 1U: <2 cm per-axis<br>• 3U – 12U: <7 cm per-axis |
| AOC-TB-17 | The facility shall include a standalone compressor for powering the air bearing for 3 hrs (2 low-Earth orbits) of continuous testing. |
| AOC-TB-19 | The air bearing disturbance torques (including friction and mass imbalance) shall have RMS values lower than:<br>• 2e-5 Nm for 1 - 6U cubesats<br>• 5e-5 Nm for 12U cubesats |

DOI: 10.13009/EUCASS2023-760



| | |
|---|---|
| AOC-TB-20 | The air bearing table shall support the following motion range:<br>• Roll/Pitch: ±30°<br>• Yaw: unlimited<br>• Roll/Pitch rates up to 5 °/s per axis<br>• Yaw rates up to 30 °/s |
| AOC-TB-21 | The facility shall have the ability to start tests with initial attitudes different from lab-horizontal (0° pitch & roll) and initial rates up to 30 deg/s. |
| AOC-TB-22 | The facility shall include independent measurements of platform orientation with fixed bias (or calibration residual) < 0.1° per-axis and attitude-dependent/time-varying error < 0.01° RMS per-axis at a sample rate of up to 10 Hz, with both latency and timestamp knowledge error (vs GSE reference) less than 0.1 s. |
| **Sensor Stimulation Requirements** | |
| AOC-TB-23 | The facility shall be capable of compensating the local magnetic field and emulating the Earth's on-orbit magnetic field with arbitrary vector direction and magnitude up to 600 uT with an error < 1 % per axis across the cubesat working area (diameter 34 cm). |
| AOC-TB-24 | The facility shall include a Sun lamp with the following properties:<br>• Angular divergence ≈ 0.53°<br>• Spatial non-uniformity < 10%<br>• Illumination working diameter ≥ 34 cm<br>• Spectral content and intensity aimed at stimulating photodiode or photocell sensors at near 1 solar constant at 1 AU<br>• A high (~1 solar constant) and low intensity option shall be present. |
| AOC-TB-25 | The Sun lamp (or Sun beam relay mirror) shall be manually moveable along a quarter-arc ranging from the overhead position to the horizontal position. |
| AOC-TB-26 | It shall be possible to emulate eclipse. |
| AOC-TB-27 | It shall be possible to optionally emulate Earth albedo (mean albedo level) only for short duration tests (where the albedo source location with respect to the s/c can be assumed static). |
| **GSE Infrastructure Requirements** | |
| AOC-TB-28 | The facility shall include real-time (hard or soft) software that is capable of:<br>• Performing the mass balancing<br>• Air bearing control (as needed)<br>• Setting simulated date and frame offset between inertial J2000 and lab frame (fixed during each test)<br>• Propagating orbit kinematics<br>• Simulating a Sun ephemeris model<br>• Estimating the platform ground-truth attitude (can include noise filtering if necessary, with cut-off higher than 10 Hz)<br>• Magnetic stimulus<br>• Star tracker stimulus<br>• Logging all relevant data from the test<br>• Real-time visualization of orbit and attitude |
| AOC-TB-32 | The facility shall include a mechanism for synchronizing on-board (satellite) time and GSE time to within 0.1 s. |
| AOC-TB-33 | The moveable platform shall include a mountable battery pack capable of supplying any GSE needs plus 30 W for 3 hrs to the satellite at a DC regulated voltage of 8, 12, 16, 18 or 24 V (all shall be supported) with maximum depth of discharge of 70% (i.e. capacity ≥ 130 W hr). |
| AOC-TB-34 | The moveable platform shall include a mountable generic communications module that connects to the cubesat via CAN (using CSP) or I2C (both shall be supported) and acts (1) as a bi-directional Telemetry & Telecommand relay with the ESA/customer-supplied ground station via wifi and (2) as a one-directional relay of star tracker template model outputs to the cubesat. |

In addition to the CubeSats listed in the requirements, the new facility will allow testing of an ADCS mock-up from Space Inventor (Aalborg, Denmark), available at ESTEC laboratory.

DOI: 10.13009/EUCASS2023-760



### 1.2. Functional Architecture

The facility functional architecture is displayed in Figure 1, where the different functions are grouped among moving and fixed equipment. Interfaces with the Cubesat under test and the GSE infrastructure are also highlighted. The fixed equipment includes the Helmholtz cage, Sun and Earth albedo lamps, the Ground truth attitude measurement system, a star tracker template model, and the Ground Support Equipment. The moving equipment includes the ABT equipped with an Automatic Balancing System (ABS), batteries and a control and communication module.
The control and communication module features wireless connectivity to serve as a one-directional relay of the star tracker template model outputs to the CubeSat. The template model is conceived as an instrument surrogate for those CubeSats equipped with star trackers and is needed as long as the facility does not enable physical stimulus for such sensors. Indeed, the inclusion of an optical stimulus device to be mounted on star trackers is foreseen as a future development.

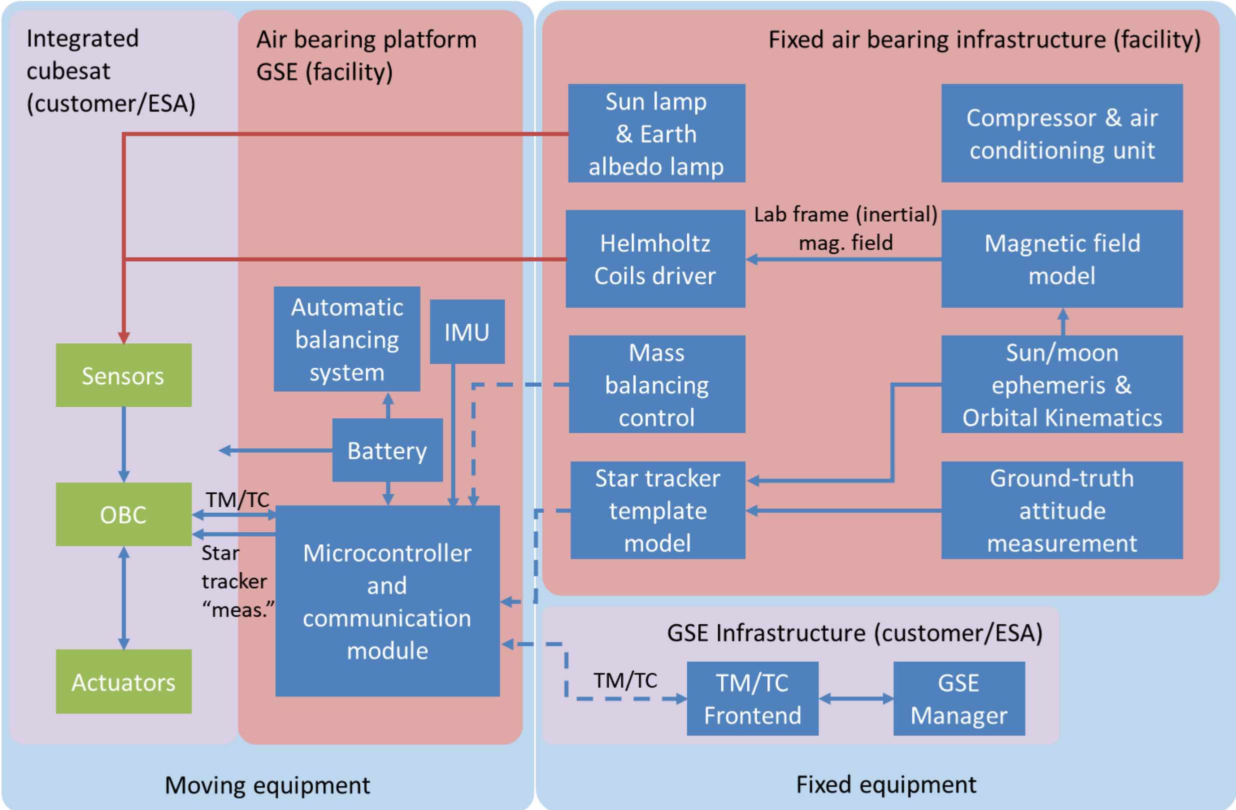


**Figure 1: Test facility functional diagram (green = satellite units, blue = GSE, blue solid lines = cabled data/power transmission, dotted lines = wireless communication, red solid lines = sensor stimulus)**

### 1.3. Facility overview

A CAD model of the facility under development is displayed in Figure 2 (right panel), in comparison with the heritage facility at the University of Bologna (left panel). From a physical layout standpoint, the major difference between the two lies in the sun-lamp re-orientation mechanism.

DOI: 10.13009/EUCASS2023-760



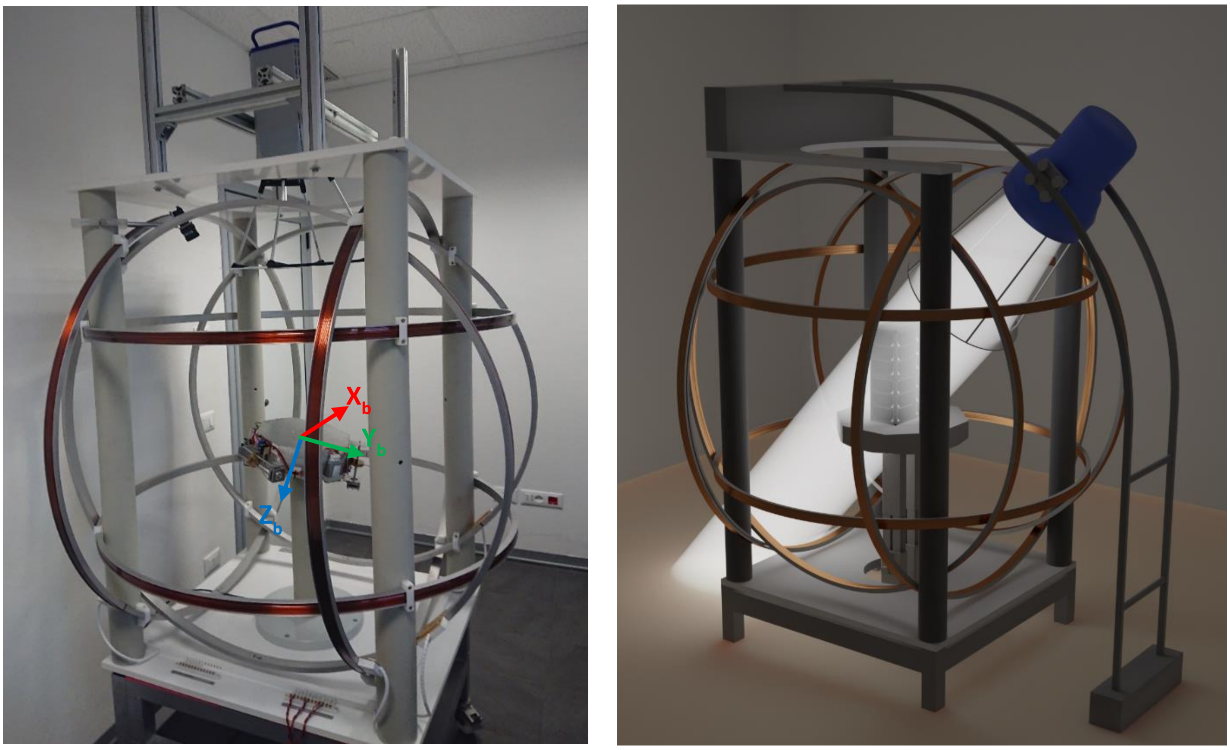


**Figure 2: Heritage facility at University of Bologna (left); updated design for ESTEC AOCS Verification Laboratory (right)**

## 2. Air Bearing Table Development

Testing of a satellite's ADCS in a space-like environment requires a (nearly) torque-free rotational motion of the satellite or of its ADCS. This can be achieved by employing a spherical air bearing, which guarantees a rotational motion with very low friction and by minimising the residual disturbance torques [3]. As a matter of fact, the gravity torque, created by the offset between the Centre of Mass (CM) and Centre of Rotation (CR) of the rotating system, is the largest torque acting on air-bearing based facilities [4]. The reduction of the gravity torque has been a big design driver in the development of the ABT and this is achieved both by designing a rigid but light platform and by using a balancing system. The air bearing is mounted on an ABT in a table-top configuration; the ABT serves as mechanical interface with the DUT and hosts, apart from the DUT itself, the ABS, batteries, the control and communication module, and other Ground Support Equipment (GSE). This kind of ABT offers some advantages: unconstrained yaw motion and the possibility of placing the DUT and other components on a unique horizontal surface. On the other hand, when using a table-top ABT counterweights are needed to balance the mass placed above the CR. In the following, the design of the new ABT is described with the CubeSats mounting system and the balancing system.

### 2.1. Air Bearing stand and Ground Support Equipment

A Commercial Off-The-Shelf (COTS) hemispherical air-bearing module (model PIglide A-653.045 from Physik Instrumente Germany) has been selected for the new facility. These kinds of air bearings are widely used for satellite attitude dynamics simulation and have already been employed in the heritage facility. They are compatible with a clean room, complying with requirement AOC-TB-02. They are manufactured in amagnetic materials (hardcoat aluminium and stainless steel), making them compatible with the use in a Helmholtz Cage. They allow a motion range of ±45° in pitch/roll and unlimited in yaw, consistently with requirement AOC-TB-20 (the actual motion range depends on the air bearing table and pedestal geometry). The air bearing is powered by a standalone low-noise compressor with a dedicated air conditioning unit.
As per requirements, the facility should support the testing of CubeSats with a wide range of mass and dimensions. A critical aspect in testing the CubeSats is the possibility of keeping their geometrical centre in the centre of the Helmholtz cage. There are different reasons for setting this requirement:

- to make sure that any DUT lies in the region of highest uniformity of the magnetic field;
- the ground-truth system relies on cameras with most of their field of view inside the Helmholtz cage area;

DOI: 10.13009/EUCASS2023-760



- the sun-lamp rail system is designed to point its light beam toward the centre of the Helmholtz cage

Thus, a pedestal with adjustable height (range 602-738 mm) has been designed to serve this scope. The pedestal includes telescopic columns and can sustain a load up to 1500 N.

A mechanical GSE is needed to lift 6U and 12U CubeSats, as per requirement AOC-TB-11. After a survey of the existing manual and electric lifters/forklifts, no COTS solution was found to satisfy simultaneously all the requirements in terms of size, load capacity, and clean room compatibility. For this reason, an electrically actuated custom lifter was designed and manufactured (Item Industrietechnik GmbH, Germany).

### 2.2. Mount platform and the CubeSats mounting system

Considering the broad range of mass and size to be tested in the facility, from 1U to 12U according to the requirements, two different mount platforms have been designed: a smaller one, that will host 1U CubeSat and the Space Inventor ADCS mock-up, plus a larger one for testing 3U, 6U, and 12U CubeSats. The design of the two platforms is adapted from the one used in the heritage facility. The size is chosen to allow placing the CubeSat mock-up, along with all the other components (balancing system, power system, electronics, etc.).

The two platforms consist of a partially hollow aluminium octagonal prism with circular and radial stiffeners. The octagonal shape, the stiffeners, and the use of aluminium allow a high stiffness-to-mass ratio of the platform, hence limiting the deformation of the platform under loading, while minimizing its mass. Increasing the stiffness of the platform is indeed important to reduce the disturbance torque due to sagging. The octagonal shape allows also the placing of the components on the prism lateral surfaces. The hollow structure allows placing the air bearing inside the platform while shifting the CM downward. Counterweights are placed beneath the platform by means of eight threaded rods.

A mounting system for the CubeSats has been designed from scratch. The mounting system allows interfacing the platform with CubeSats of different sizes with contact occurring only at their rails, as specified in the requirements. The mounting system relies on aluminium guiderails, similar to those found in a CubeSat deployer, with Teflon inserts to prevent aluminium-to-aluminium contact between the CubeSats rails and the guiderails.

### 2.3. Balancing system

The balancing system is aimed at reducing the CM to CR distance such that the gravity torque is minimised. The accuracy achievable in the compensation of the CM to CR offset is inversely proportional to the mass used in the balancing system. For this reason, the balancing procedure is divided into two steps: coarse balancing and fine auto-balancing. The former has the goal of compensating for the macroscopic offset between CR and CM using counterweight masses mounted on the main platform through 8 threaded bars placed beneath it. In the second the position of the CM is brought a few micron distance from the CR using little masses (a few hundred grams) moved by stepper motors.

The coarse balancing procedure requires the sizing of the counterweights based on the expected value of the mass of the DUT and of the position of its CM with respect to its geometrical centre. These parameters can vary within the limits specified by requirements AOC-TB-15 and AOC-TB-16 so a unique value of mass for the counterweights cannot fit all the cases. Instead, limit values for the CubeSats mass and CM envelop are considered and the corresponding sizes of counterweights are determined. In this way coarse balancing can be achieved, both in the limit and intermediate cases. The value of the counterweights' mass is determined by (1), obtained by imposing the balancing of the first moment of mass around the CR. $m_c$ is the total mass of the counterweights, $r_c$ is the distance of the counterweight's CM from the CR, $m_i$ is the mass of the $i^{th}$ component and $r_i$ the relative distance of the CM from the CR.

$$m_c = \frac{\sum m_i r_i}{r_c} \tag{1}$$

Balancing in the vertical direction is the most critical in terms of offset between CM and CR. Table 2 reports the mass and CM position of the components giving the main contribution to the mass balancing and the needed counterweights' mass for each limit case. The extreme cases in which the satellite mass and CM position are at their maximum and minimum values are considered since they are the ones requiring the highest and lowest counterweight's mass. Vertical and horizontal orientations refer respectively to the cases in which the CubeSat is placed on the mount platform with its smallest and largest face parallel to the platform plane. The additional GSE is assumed to be placed on the platform plane.

DOI: 10.13009/EUCASS2023-760



**Table 2: evaluation of counterweight mass needed for the different CubeSat mass and CM location scenarios**

| Case N. | DUT | Orientation | DUT mass [kg] | DUT CM to geometrical centre offset [mm] | Additional GSE | Counterweights mass [kg] |
|---|---|---|---|---|---|---|
| **1** | CubeSat 1U | Vertical | 2 | + 20 | Yes, 2 kg | 1.7 |
| **2** | CubeSat 1U | Vertical | 1 | - 20 | No | 0* |
| **3** | CubeSat 1U | Horizontal | 2 | + 20 | Yes, 2 kg | 1.3 |
| **4** | CubeSat 1U | Horizontal | 1 | - 20 | No | 0* |
| **5** | Space Inventor ADCS mock-up | / | 2 | / | Yes, 2 kg | 0.2 |
| **6** | CubeSat 3U | Vertical | 6 | + 70 | Yes, 2 kg | 9.8 |
| **7** | CubeSat 3U | Vertical | 3 | - 70 | No | 1.0 |
| **8** | CubeSat 3U | Horizontal | 6 | + 20 | Yes, 2 kg | 2.6 |
| **9** | CubeSat 3U | Horizontal | 3 | - 20 | No | 0* |
| **10** | CubeSat 6U | Vertical | 12 | + 70 | Yes, 2 kg | 20.2 |
| **11** | CubeSat 6U | Vertical | 6 | - 70 | No | 5.8 |
| **12** | CubeSat 6U | Horizontal 1 | 12 | + 45 | Yes, 2 kg | 14.4 |
| **13** | CubeSat 6U | Horizontal 2 | 6 | - 20 | No | 1.0 |
| **14** | CubeSat 12U | Vertical | 24 | + 70 | Yes, 2 kg | 33.2 |
| **15** | CubeSat 12U | Vertical | 12 | - 70 | No | 12.2 |
| **16** | CubeSat 12U | Horizontal | 24 | + 45 | Yes, 2 kg | 24.2 |
| **17** | CubeSat 12U | Horizontal | 12 | - 45 | No | 7.4 |

*no counterweights needed in this case, the mass of the mount platform is sufficient to balance the mass of the satellite

The counterweights mass can be distributed on the 8 threaded bars of the mounting platform and their position can be adjusted to get a more accurate balancing. Balancing in the horizontal direction can be achieved by distributing the same amount of mass unevenly on the bars. Overall, counterweights of mass in between 0.050 kg and 2.000 kg will be employed. The goal of the coarse balancing system is to bring the CM to a distance from the CR that can be compensated by the fine balancing system. This distance has been set to 1 mm as a compromise between the accuracy required by the coarse balancing system (and hence the effort in executing it) and the accuracy of the fine balancing system which in turn determines the smallest residual torque acting on the facility.

The fine balancing system is based on a two-step procedure consisting of a real-time compensation of the X-Y (in-plane) components of the CM to CR offset vector followed by the estimation of the residual Z-component (see Figure 2 for a definition of the ABT axes). Three mutually orthogonal stepper motors carry three balancing masses and are remotely controlled. The procedure, described in detail in [5], is summarised hereafter.

For the in-plane automatic balancing, the mass position vector, $\boldsymbol{r}_b$, commanded to the stepper motors is computed according to:

$$\boldsymbol{r}_b = \frac{\boldsymbol{g} \times \boldsymbol{\tau}_u}{\| \boldsymbol{g} \|^2 \, m_b} \tag{2}$$

where $\boldsymbol{g}$ is the gravitational acceleration vector, $m_b$ is the balancing mass, and $\boldsymbol{\tau}_u$ is the desired control torque. The latter is computed as:

$$\boldsymbol{\tau}_u = -K_\mathrm{p}\hat{\mathbf{g}} \times \hat{\mathbf{z}} - K_\mathrm{d}\boldsymbol{\omega}_\mathrm{p} - K_\mathrm{d}K_\mathrm{I}\int_0^t K_\mathrm{p}\hat{\mathbf{g}} \times \hat{\mathbf{z}}\mathrm{d}t \tag{3}$$

where $K_\mathrm{p}$, $K_\mathrm{d}$, $K_\mathrm{I}$ are the gains of the control law, $\boldsymbol{\omega}_\mathrm{p}$ is the projection in the horizontal plane of the angular velocity vector and $\hat{\mathbf{z}}$ is the third body axis, normal tot the rotating platform surface. In essence, the feedback control law acts to suppress the in-plane components of the gravity vector, thereby aligning the Z-body axis to the local vertical.

Afterward, the inertia matrix and the vertical component of the CR to CM vector are estimated by sampling of the free-platform oscillations through gyro readings. Assuming the oscillations to be driven by the rigid body dynamics under the influence of the gravity torque alone, the estimation problem can be formulated as a constrained least squares minimization, with the unknown vector including the inertia matrix elements plus the CR-to-CM Z-offset, and the constraint lying in the prescribed zero values of the X-Y offset components (the full equations can be found in [5]). Once the Z-offset is estimated, the Z-balancing mass position is adjusted accordingly.

DOI: 10.13009/EUCASS2023-760



The minimum torque that can be compensated by the fine balancing system depends on the accuracy with which the balancing mass can be moved and on the value of the mass itself. The first is determined by the stepper motors resolution, usually expressed in mm/steps. The ABT is equipped with a set of stepper motors with integrated linear guides (Dings' DLM Series). Two different sizes for the motor frame are used in the 1U and 3U-12U platform. The characteristics of both models are summarised in Table 3. The stroke length has been selected according to the mount platform size and the expected offset between CR and CM after coarse balancing.

**Table 3: Stepper motors specifications**

| Model name | Motor frame size | Travel per step @ 1.8° [mm] | Stroke length |
|---|---|---|---|
| **DINGS' DLM28** | 28 mm | 0.001600 | 150 mm |
| **DINGS' DLM42** | 42 mm | 0.003048 | 250 mm |

For sizing the masses to be used for the fine auto-balancing, some worst-case balancing scenarios are considered, which occur when the CubeSat is mounted in vertical orientation and its CM is located at the uppermost position allowed according to the CubeSat design specifications, see Table 2. The computation assumes that the platform mass minus the ABS mass with an assumed CR to CM distance can be balanced by a sliding mass at a distance equal to half the linear actuator stroke length. The theoretical residual torque is calculated as the product of the sliding mass, the stepper motor travel per step and the acceleration of gravity. The result of the sizing is summarized in Table 4.

**Table 4: balancing mass sizing**

| CubeSat | Total mass minus the ABS mass [kg] | Max. CR to CM offset after coarse balancing [m] | Linear actuator stroke size/2 [m] | ABS mass [kg] | Travel per step [mm] | Theoretical residual torque [Nm] |
|---|---|---|---|---|---|---|
| **1U** | 11.424 | 0.001 | 0.075 | 0.152 | 0.000001600 | $2.39\ 10^{-6}$ |
| **3U** | 30.916 | 0.001 | 0.125 | 0.247 | 0.000003048 | $7.39\ 10^{-6}$ |
| **6U** | 48.470 | 0.001 | 0.125 | 0.388 | 0.000003048 | $1.16\ 10^{-5}$ |
| **12U** | 73.917 | 0.001 | 0.125 | 0.591 | 0.000003048 | $1.77\ 10^{-5}$ |

The auto-balancing step is implemented using an Adafruit Feather M0 board with integrated WiFi, which processes the data gathered from an XSens Mti 3.0 IMU through I2C communication. The onboard microcontroller communicates with the ground via WiFi through the User Datagram Protocol (UDP).. The microcontroller acts also as a bidirectional relay between the ground station and the CubeSat, to which is connected using a dedicated CAN module. A graphical user interface (GUI) is available on the ground side to monitor the balancing procedure, see Figure 3. Through the GUI the user can:

- Start/Stop the mass balancing process
- Set an arbitrary position for the stepper motor masses
- Change the automatic balancing control law's gains
- Estimate the inertia of the platform, CM to CR offset and residual disturbance torque
- Visualise attitude and attitude rate data read from the on-board IMU
- Collect data of the balancing process and saving it to a txt/csv file

A test plan has been prepared aimed at verifying the performance achieved by the balancing system across the whole range of sizes and configurations of CubeSat platforms.

DOI: 10.13009/EUCASS2023-760




**Figure 3: Mass balancing GUI**

## 3. Physical Stimulus Development

Thanks to its PS subsystems, the facility will allow testing of the most common sensors employed on CubeSats, such as magnetometers and Sun sensors and, in a future development (not included in this project), star trackers. A Helmholtz cage is used to simulate the magnetic field that the satellite will experience in Low Earth Orbit (LEO), with optional magnitude scaling to increase the magnetic actuators control authority. The magnetic field simulator is described in 3.1. A ground-truth system, described in 3.2 is used to gather independent ground-truth attitude estimate and to provide input to a star tracker template model. Sun sensors are stimulated by a sun simulator with adjustable orientation, described in 3.3.

### 3.1. Magnetic field simulator

A tri-axial Helmholtz cage can be used to simulate the Earth geomagnetic field in a LEO, with simulation of both intensity and direction of the magnetic field measured by the spacecraft based on its simulated position. The generated magnetic field can be eventually scaled in intensity and in frequency to allow compensating for the effect of disturbance torques. Given the size constraints set by requirements, the heritage Helmholtz cage has been considered as a baseline for the first design iteration, namely, a Ferronato® BH-1300-3-C from Serviciencia, Spain. It features three orthogonal pairs of coils (D ≈ 1300 mm) that can generate an arbitrary magnetic field in the range ±10 Gauss. Magnetic field in-homogeneity is below 1% (5%) in a spherical volume of 404 (586) mm in diameter, concentric with the coil pairs, which is compliant to requirement AOC-TB-23. The nominal field-to-current ratio is 50.5 µT/A, ±1%. A power supply is used to power the coils of the Helmholtz cage and a relay is used for bipolar current control. The desired magnetic field is mapped into the Helmholtz coils' current by an Arduino board that controls a relay. The board reads the magnetic field components from the magnetometer and computes the current to be sent to the coils based on the commanded magnetic field. A magnetometer is used to read and compensate for the environmental magnetic field.
To meet the need for a facility re-location via wheels (AOC-TB-14) and the 195cm height limit (AOC-TB-13), a customized support table equipped with lockable castors and reduced height has been designed. An important difference with respect to the heritage design consists on the fact that the air bearing pedestal now lies directly on the ground rather than being placed on the Helmholtz cage structure. This allows to relax the requirements in terms of admissible load on the Helmholtz cage support table and hence reduce its height.

DOI: 10.13009/EUCASS2023-760



### 3.2. Ground-truth system

To estimate the true attitude of the mock-up under test, the facility will be equipped with an independent ground-truth attitude system as per req. AOC-TB-22. Although the heritage facility embedded an in-house monocular vision system for ground truth, its current capabilities do not match the requirements, which led to the choice of a COTS OptiTrack 6DoF tracking system (NaturalPoint, Inc. DBA OptiTrack, USA), relying on calibrated cameras equipped with 850 nm band-pass filter. In addition to providing ground truth attitude, the tracking system will fed a template star tracker model. This last provides quaternion measurements to the CubeSat on-board computer as if they were gathered by the star tracker itself, by converting the ground-truth attitude into inertial-to-star-tracker quaternion based on user-specified alignment quaternion and optional band-limited white noise.
A preliminary version of the ground truth system has been procured as part of an upgrade of the heritage facility at the University of Bologna. It is configured as a dual wide-FoV (Field of View) (79°×47°) camera set tracking passive spherical markers (see Figure 4). The performance of a motion capture system is typically rated in terms of reconstructed 3D markers position accuracy, which is expected to be better than 0.2 mm in small volumes typical of our application. Such an error, however, cannot be directly translated into attitude accuracy, thereby a test campaign is being performed to check the suitability of the selected tracking system for the ESTEC facility.

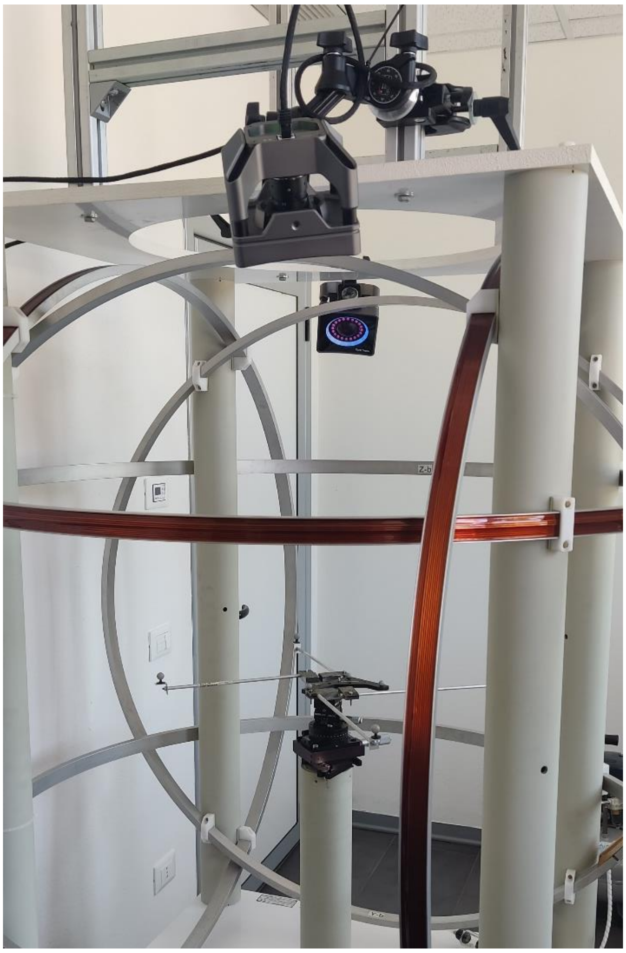

**Figure 4: Test set-up for the ground-truth vision system prototype.**

### 3.3. Sun simulator

A Sun simulator is required for the facility to act as a stimulus to Sun sensors carried onboard the device under test. A Sun simulator is classified according to three criteria, namely: (a) spectral matching, (b) spatial uniformity, and (c) temporal stability. For testing a Sun sensor, other parameters are of importance, such as the collimation of the light beam over a wide area, that shall be maintained close to 0.53° i.e., the apparent angular diameter of the Sun at 1 AU, and the power flux level (1367 W/m$^2$ at 1 AU) at the nominal target distance. According to req. AOC-TB-24, the Sun simulation shall feature the following properties:

DOI: 10.13009/EUCASS2023-760



i. Angular divergence ≈ 0.53°
ii. Spatial non-uniformity < 10%
iii. Illumination working diameter ≥ 34 cm
iv. Spectral content and intensity aimed at stimulating photodiode or photocell sensors at near 1 solar constant at 1 AU. A high (~1 solar constant) and low intensity option shall be present.

The first two performance indexes were achieved in the heritage facility, by making use of a daylight LED studio source. In that case, the required degree of light collimation was achieved (on a smaller area than required in *iii*) thanks to a custom collimating Fresnel lens mounted at about 40 cm distance from the source. We adopted the same collimating lens concept for the ESTEC facility.

LED lamps are known for not providing good spectral matching out of the visible spectrum, lacking substantial output in the UV and IR bands. This is why other sources are usually employed in Sun simulators, such as Xenon or Metal Halide (HMI) lamps. The latter are in particular often used in studio lighting to provide "natural" resembling solar illumination. Even though the higher spectral matching of HMI is a desirable feature, the significant (Near Infrared) NIR output leads to some drawbacks as: i) overheating problems to the DUT and ii) larger disturbance to the ground truth vision system, whose cameras are sensitive in a NIR band centered at 850nm. As a result, although a HMI lamp was initially evaluated and tested for being used a solar simulator in the facility (see Figure 5), it was eventually discarded in favor of a LED.

Such a choice is also supported by the observation that most European Sun sensors are based on photodiodes whose sensitivity spectrum is dominated by the visible band.

To size the simulator, given that the DUT will lie at a distance not larger than 1m from the illumination source, a LED rated at 600 W is enough to achieve 1 solar constant (≈1370 W/m$^2$) over the illumination working diameter (surface area of ≈0.1m$^2$) as long as the light collection efficiency of the collimator is higher than 137W/600W ≈ 23%.

The Sun simulator orientation can be adjusted along a quarter-arc ranging from the overhead position to the horizontal position, thanks to a double track curvilinear rail with roller sliders (see Figure 2, right panel), whose detailed design is ongoing. This way, different *solar beta angles* can be simulated for satellites whose attitude is locked to the orbit-frame.

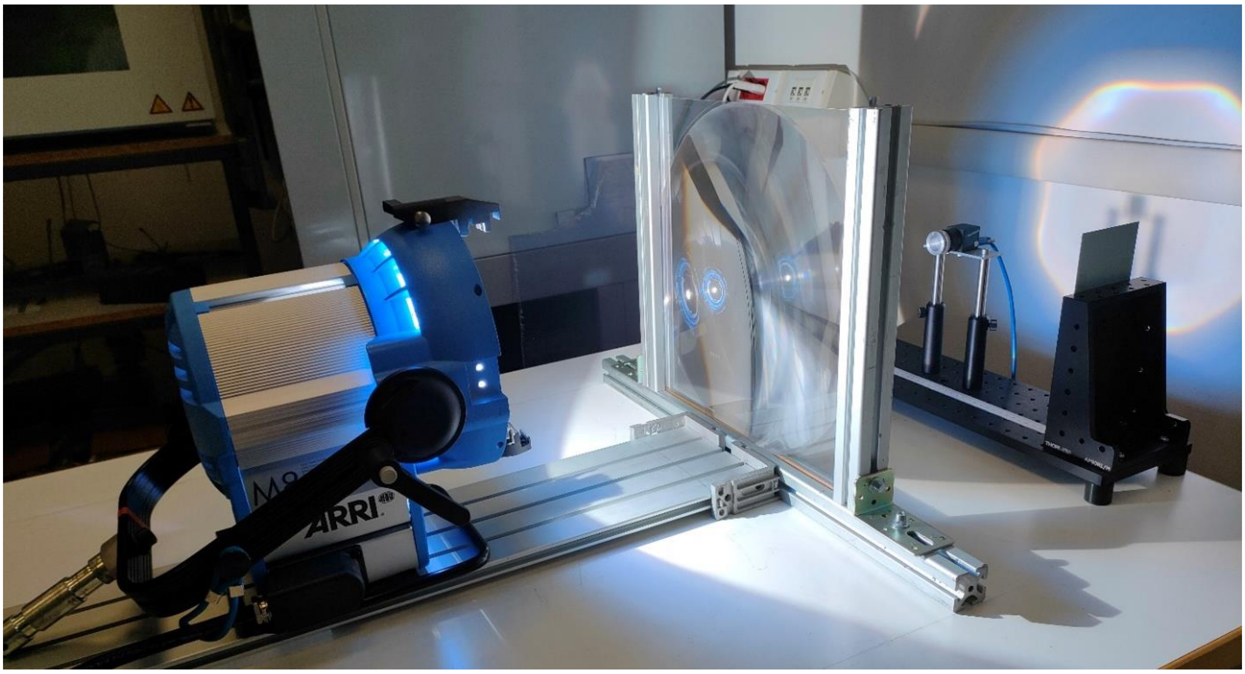


**Figure 5: Solar simulator testbed with a COTS light source, a Fresnel lens, and a pinhole camera detector for verification of light-beam uniformity and divergence**

## Conclusions

Due to the increasing popularity of nanosat/CubeSat platforms in ESA missions, the Agency has a strong interest in adopting a verification and validation facility to reduce mission failures which often occur due to issues with the ADCS in-flight. To this end, a 3-DOF attitude control air-bearing facility, currently being designed and manufactured jointly by Nautilus Navigation in Space Srl and the University of Bologna under ESA contract, will be installed at the AOCS Verification laboratory in ESTEC. The new facility, based on a heritage development described in [2], will improve

DOI: 10.13009/EUCASS2023-760



upon its predecessor from several points of view, most notably by allowing to test a wide range of CubeSats, from 1U to 12U, in any mounting orientation. In this manuscript, we reported on the current project status, starting from the main design drivers and the solutions adopted to meet the requirements. A first milestone will be achieved through the verification tests of the ABT performance, to be held by September, while the project is expected to culminate with the facility commissioning by the end of 2023.

Eventually, the new facility will hopefully serve as a key tool to enhance the success rate of the next-generation ESA-led CubeSat missions.

## References

[1] European Space Agency, '3DOF Attitude Control Air Bearing Facility. Statement of Work ESA-TECSAA-SOW-2022-002591.', 2022.

[2] D. Modenini, A. Bahu, G. Curzi, and A. Togni, 'A Dynamic Testbed for Nanosatellites Attitude Verification', *Aerospace*, vol. 7, p. 31, Mar. 2020, doi: 10.3390/aerospace7030031.

[3] J. Schwartz, M. Peck, and C. Hall, 'Historical Review of Air-Bearing Spacecraft Simulators', *Journal of Guidance, Control, and Dynamics*, vol. 26, May 2003, doi: 10.2514/1.1035.

[4] R. C. Da Silva, R. A. Borges, S. Battistini, and C. Cappelletti, 'A review of balancing methods for satellite simulators', *Acta Astronautica*, vol. 187, pp. 537–545, Oct. 2021, doi: 10.1016/j.actaastro.2021.05.037.

[5] A. Bahu and D. Modenini, 'Automatic mass balancing system for a dynamic CubeSat attitude simulator: development and experimental validation', *CEAS Space Journal*, vol. 12, no. 4, pp. 597–611, Dec. 2020, doi: 10.1007/s12567-020-00309-5.